STARJET: PNEUMATIC DISPENSING OF NANO- TO PICOLITER DROPLETS OF LIQUID METAL

T. Metz[1], G. Birkle[2], R. Zengerle[1,2], and P. Koltay[2]
[1]HSG-IMIT, Villingen-Schwenningen, GERMANY
[2]IMTEK - University of Freiburg, Freiburg, GERMANY

ABSTRACT

In this work we present a novel, simple and robust, pneumatically actuated dispenser for nano- to picoliter sized droplets of liquid metals. The so called StarJet dispenser utilizes a star-shaped nozzle geometry that stabilizes plugs of liquid in the centre of the nozzle by capillary force. This minimizes the wall contact of the liquid plug and reduces contact line friction. Individual droplets of liquid metal can be pneumatically generated by interplay of the sheathing gas flow in the outer grooves of the nozzle and the liquid metal. The working principle was first discovered and studied by Computational Fluid Dynamic (CFD) simulations. For experimental validation silicon chips with the star-shaped geometry were fabricated by Deep Reactive Ion Etching (DRIE) and assembled into a printhead. With different nozzle chips volumes between 120 pl and 3.6 nl could be generated at natural frequencies of 90 Hz and 400 Hz. The StarJet can either be operated as drop on demand or as continuous droplet dispenser. We printed columns of metal with 0,5 to 1,0 mm width and 40 mm height (aspect ratio >40) to demonstrate the directional stability of the ejection.

INTRODUCTION

The contact free dispensing of tiny liquid volumes in the nano- to picoliter range is an important application field for MEMS technologies since more than twenty years, from inkjet printing [1], to the printing of microarrays [2] and for rapid prototyping methods [3]. A particularly challenging area is the dosage of liquid metals [4]. This is required for the generation of solder bumps [5] for flip chip bonding or for rapid prototyping of electric circuits [3] and metallic devices. Further the dosage of small droplets to arm MEMS fabricated mercury switches [6] is of interest.

The contact free dispensing of liquid metals is challenging for different reasons: The dosage device must operate above the typically high melting temperatures of the metal. The high temperatures and the temperature changes during heating and cooling can induce mechanical stress that complicates assembly of the devices and boosts oxidation. Preventing oxidation of the jetted droplet is an additional issue. Therefore a constant flow of inert gas around the liquid metal is required. If the droplet generators are driven by piezo ceramics [4], the piezos must be thermally insulated as their working range is limited by the Curie temperature that ranges normally between 150°C and 300°C. Finally, the high surface tension of liquid metals prohibits capillary priming of devices as it leads to very high contact angles on most materials.

The StarJet system presented in this work is a rather simple solution for the dosage of liquid metals and does not suffer from any of these problems. It applies the sheet gas flow required to prevent oxidation as actuation mechanism and takes advantage of the high contact angles between the liquid metal and the nozzle chip fabricated of silicon. The assembly of the nozzle chip into the printhead is kept simple so thermal stresses do not affect the system.

WORKING PRINCIPLE

The heart of the StarJet dispenser is a star shaped nozzle as shown in Fig 1a. The profile was first studied as geometry for minimizing gas bubble resistance in tubes [7] (StarTube). For the dispensing of liquid metals the nozzle is fabricated from silicon to provide thermal stability and a high contact angle ($\theta > 150°$) towards the liquid metal. In Fig. 2a/b SEM pictures are shown of the top and the interior of a StarJet nozzle chip fabricated by DRIE within this work. The star shaped nozzle profile leads to a centering of a droplet or plug of liquid metal in the nozzle as shown by a simulation using CFD [8] in Fig. 1b.

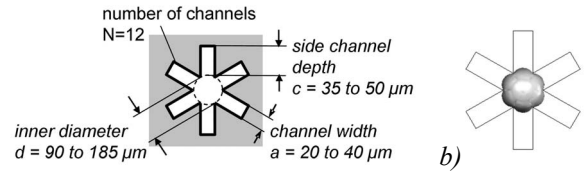

Figure 1: a) Schematic cross section of the star shaped nozzle. b) CFD simulation showing the centered droplet in the star shaped nozzle.

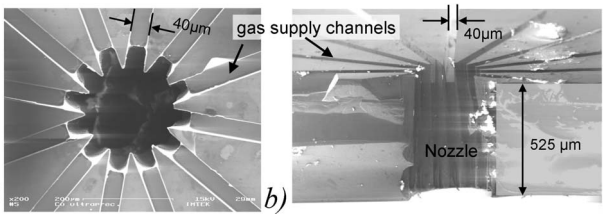

Figure 2: SEM pictures of fabricated StarJet nozzle chips

The droplet generation mechanism in the StarJet is explained in Fig. 3. It is somewhat similar to the droplet or bubble generation in a flow focusing device [9]. The liquid reservoir is placed directly above the inlet of the nozzle chip. The inner surface of the nozzle chip features gas supply channels (Fig. 2). These channels enter the nozzle in the side grooves of the star shaped profile. The liquid reservoir and the gas supply channels are in fluidic contact as shown in Fig. 3. When applying a pressure to the common inlet at top of the StarJet system, a gas flow through the gas supply channels is induced with a pressure drop Δp along the gas supply channels (Fig. 3a).

If this pressure drop Δp is high enough to overcome the capillary pressure of the nozzle centre, a liquid plug is forced into the star shaped nozzle since the driving pressure also acts on the liquid metal in the reservoir (Fig. 3b).

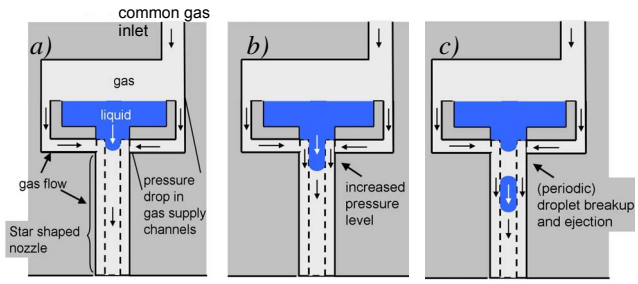

Figure 3: Working principle of the StarJet dispenser

As stated above, the liquid plug is confined in the center of the nozzle by capillary forces and the gas flow can still hold on in the outer grooves of the star shaped profile.

In response to the liquid plug entering the nozzle the gas flow resistance increases and the pressure level in the nozzle (Fig. 3b) raises. Like in an electrical voltage divider the pressure drop across the supply channels decreases. Therefore the liquid column collapses at the point of highest pressure near to the connection point of the gas supply channels. While the liquid column becomes necked a gas flow induced force onto the separating droplet towards the outlet supports the breakup. Finally the droplet is transported with the gas flow out of the nozzle (Fig. 3c). Until the droplet is ejected, the liquid column can not reenter the nozzle. Thus the system provides self controlled single droplet breakup. After ejection the sequence restarts.

A key feature of the StarJet dispenser is that the star-shaped profile reduces wall friction of droplets. This supports the transport decisively and reduces deflecting forces during ejection. The driving sheet gas protects the hot metal from oxidation as droplets during the generation and during free flight but also at rest in the reservoir by constantly rinsing the system at a low pressure level.

THEORY

Star shaped nozzle

A droplet is centered in the star shaped nozzle profile if the repellent capillary pressure of the outer fingers is too high for the droplet in the centre to move into the outer fingers. The effect depends on the number of fingers that form the nozzle and the wetting angle between the nozzle material and the liquid to be transported. The critical number of fingers necessary to enable a centered droplet in dependence of the contact angle is given in the condition Eq. (1) that is illustrated in Fig. 4. Further details and a derivation of Eq. (1) are given in [7]

$$N > \pi \left(\arctan\left(\frac{2\cos^2\theta}{2\theta - \pi - 2\cos\theta\sin\theta} \right) \right)^{-1} \qquad (1)$$

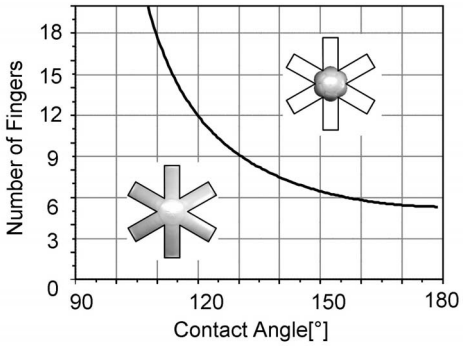

Figure 4: Number of side channels (fingers) required for centered droplets as function of the wetting angle.

Minimum actuation pressure

The minimum pressure difference Δp_{min} necessary to force a liquid column into the StarJet nozzle can be estimated by the inner diameter d of the nozzle (Fig. 1). The contact angle is virtually 180° as nearly no wall contact exists and the capillary pressure p_{cap} can be calculated from the surface tension σ of the liquid only by Eq. (2):

$$\Delta p_{\min} > p_{cap} = \frac{4}{d}\sigma \qquad (2)$$

As discussed above Δp_{min} has to drop along the gas inlet channels.

SIMULATIONS

The mechanism of droplet breakup was first studied by computational fluid dynamics (CFD) simulations using the software package CFD-ACE+ [8]. It allows the solution of the Navier-Stokes equations for two different fluids under consideration of surface tension and contact angles. In the simulation only the interior of the star shaped nozzle is considered with simplified boundary conditions: Where the gas supply channels enter the nozzle a constant gas flow is set. At the interface between liquid reservoir and nozzle a liquid inlet with a constant

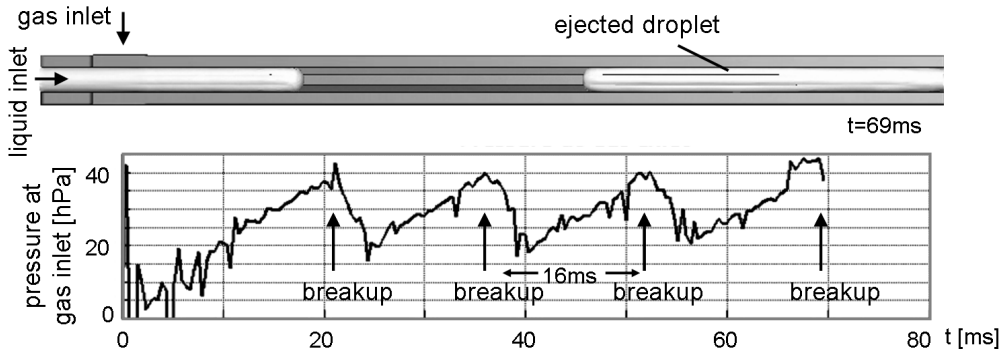

Figure 5: Result of CFD simulation with simplified model shows a periodic pressure signal at the gas inlet corresponding to a periodic droplet breakup. Boundary conditions: Constant pressure at liquid inlet (p=120hPa; mercury:$\rho = 1350 kgm^{-3}$; $\sigma = 484\ Nm^{-1}$; $\eta = 1{,}55$ Pa s) and constant velocity at gas inlet (1 ms^{-1}, air) (Outlet: ambient pressure).

pressure boundary condition is applied. Despite the constant boundary conditions the liquid column that enters the nozzle periodically breaks into plugs once the pressure gradient along the plug overcomes a critical threshold value as shown in Fig. 5.

FABRICATION

Chip fabrication

Nozzle chips were fabricated by etching the star-shaped nozzle profile and the gas channels into a 525 µm thick silicon wafer (Fig. 2). A thermal oxide layer was first structured with the geometry for the gas supply channels. The oxide layer was then covered by a resist film that was structured with the star shape. The nozzle profile was etched by DRIE into the wafers up to a residual thickness of 80 µm. The rest of the nozzle and the gas supply channels were etched using the oxide mask. The complete chip design additionally contains etched pin holes that serve for the alignment of the chips within the printhead. From Fig. 2a one can find that the etching of the star shaped profile is not perfectly straight but the inner diameter increases towards the outlet. This is caused by the DRIE process, but is not preventing the desired effect. In principle the tapering adds some additional pressure force onto the droplet breakup due to the narrowing of the gas channels.

Twenty different designs with parameters as defined in Fig. 1 were fabricated within one mask set. After examination of fabrication quality and some primary tests, two chip designs (SJet2, SJet14) were selected for experimental studies. The dimensions of these chips are given in Table 1 together with those used in the simulation shown in Fig. 5. The chip design named SJet14 has twice the central diameter d as the one named SJet2. The value p_{cap} is calculated according to Eq. 2.

Table 1: Parameters of StarJet nozzles studied.

	SJet2	SJet14	simulation
N	12	12	8
a [µm]	20	40	76
c [µm]	35	50	87
d [µm]	94	188	100
p_{cap} [hPa]	197	99	100

Experimental Setup

The printhead fluidically connecting the chips was designed as shown in Fig. 6 and fabricated in brass by milling. It was heated by a soldering iron and contains a solder reservoir and a gas inlet port for the pneumatic actuation. The nozzle chips are mechanically clamped into the printhead. A drilled hole in the center (Ø 400 µm) connects the reservoir to the liquid inlet of the chip. The alignment of the central hole is not critical as the same condition that prevents the liquid metal from moving into the outer channels of the star shaped profile protects the gas supply channels of the chip from being clogged by the liquid metal.

An external solenoid valve controls the gas flow of nitrogen supplied for pneumatic actuation. The valve switches between a low pressure level (50 hPa) for constant rinsing with sheet gas and an adjustable higher pressure level to actuate the system. The temperature is controlled during the experiments with a thermocouple near the chip and was set to 255+/-5°C. For the observation of droplets the setup was placed in front of a stroboscopic camera as shown in Fig. 7. A microphone capsule in the pneumatic supply tubing was used to determine pressure disturbations during droplet breakup. In all experiments solder of grade Sn60Pb (ρ = 860kgm^{-3}; σ = 460 Nm^{-1}; η = 2 Pas at 255°C; T_{liq}~190°C), was used.

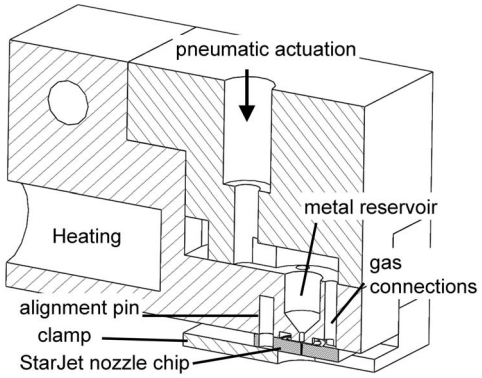

Figure 6: Design of the printhead used to heat and to fluidically connect the nozzle chips.

EXPERIMENTS

Experiments were performed with the two nozzle chips SJet2 and SJet14 to study the working principle. For a number of different pressure levels, the droplet size and breakup frequencies were studied. The minimum actuation pressure Δp_{min} was found to be 150 hPa for the larger nozzle SJet14 and 400 hPa for the smaller nozzle SJet2.

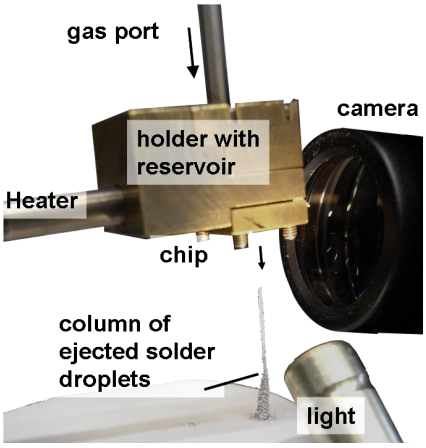

Figure 7: Photograph of the experimental setup.

When actuation with a static pressure a periodic droplet breakup could be observed like expected. In Fig. 8 stroboscopic pictures of the droplet breakup are shown. From these pictures it can be found that the solder leaves the nozzle already as preformed droplets. This proofs that the droplet breakup takes place already inside the nozzle.

The frequencies of droplet breakup were investigated from the signals recorded by the microphone. As shown in Fig. 9 the waveform is regular and periodic. For both chips the breakup frequencies close to Δp_{min} were determined to be around 95 Hz with a reproducibility of +/-15Hz. In single experiments the bandwidth was around +/- 3Hz.

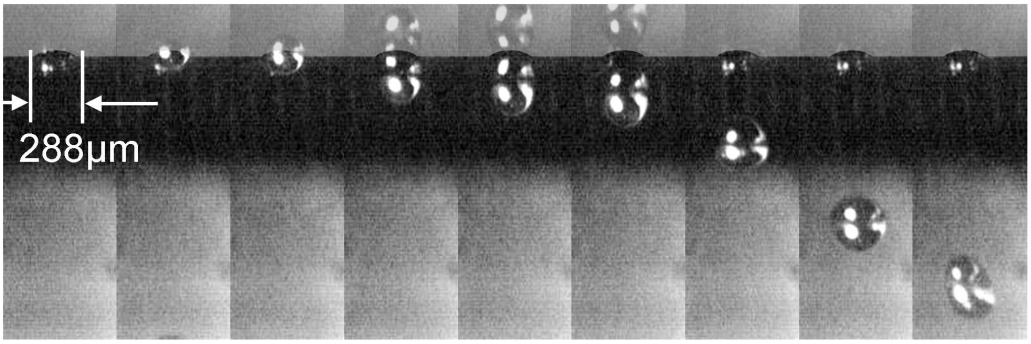

Figure 8: Stroboscopic pictures of droplet ejection are shown. Every picture relates to a new droplet.

For the SJet14 chips the frequency of the droplet breakup has been found to be stable up to 300 hPa. A further increase of the driving pressure raised the dispensing frequency strongly up to 400 Hz. When further increasing the pressure level towards 1500 hPa for SJet14 and towards 2000 hPa for SJet02 the system behavior changed towards spraying with a finite cone. For such high pressures the dynamic pressure in the gas flow becomes dominant and the described droplet generation principle fails.

By single actuation of the valve for only 6 ms with 200 hPa for Sjet14 dispensing of single droplets in a drop-on-demand mode could be achieved.

The size of droplets generated close to the minimum actuation pressure was determined by SEM pictures (Fig. 10). Due to the high heat capacity of the solder, the droplets do not solidify during flight but when meeting the substrate and get flattened. In contrast, nearly spherical droplets that do not merge could be achieved by dispensing from a distance of 30 cm into a water/soap mixture. The droplet diameter corresponds well to the inner diameter of the StarJet nozzles (Fig. 10). Droplet volumes were evaluated to be 120 pl and 3.6nl for SJet02 at 600 hPa and SJet14 at 200 hPa.

The columns built up during periodic dispensing on a constant position indicate the scattering of the droplets. Even for a height of up to 30 mm their width was only between 500 µm and 1 mm demonstrating the directional stability of the system. A reason for this might be the rather low contact area between droplet and nozzle chip. This prevents frictional forces at the nozzle outlet to deflect the ejected droplet.

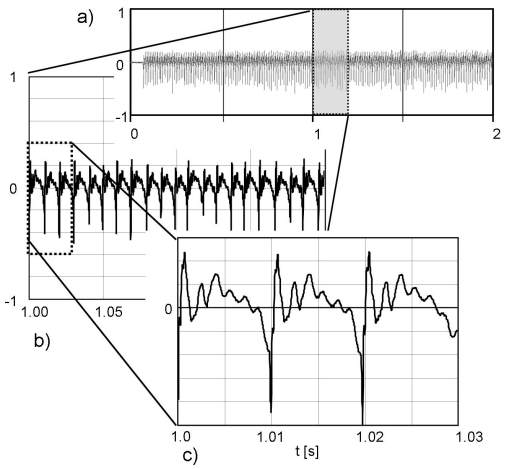

Figure 9: Acoustic signal of droplet breakup: a) full signal; b) zoom into 200ms of signal; c) zoom into 30ms of signal (SJet14, actuation pressure 150 hPa).

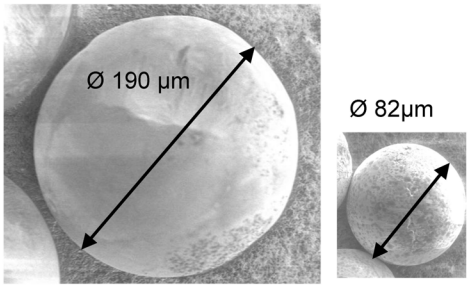

Figure 10: SEM pictures of droplets when dispensed from 30 cm distance into soap water.

CONCLUSIONS

The StarJet dispenser as presented in this work exhibits a new concept for droplet dispensing by pneumatic actuation that fits well to the requirements of the dosage of liquid metal. It is a promising principle for applications in this field. A prototype of the StarJet dispenser and a MEMS based fabrication process were successfully established. The working principle is basically understood. Three different working modes were found: continuous droplet generation, drop on demand and spray. The modes depend on the actuation pressure and duration which are externally controllable. The application of the StarJet dispenser must not be limited to liquid metal but can be applied to other liquids like aquaous solutions if nozzles are fabricated that meet the conditions given by Eq. 1 and Fig. 4 for that specific liquid.

REFERENCES

[1] J. Heinzl and C. H. Hertz, *Adv. Imag. Elec. Phy.*, vol. 65, pp. 91-171, 1985

[2] B. de Heij et al., *Anal. Bioanal. Chem.*, vol. 378, no. 1, pp. 119-122, Jan.2004

[3] M. Ession, et al., CA000002373149A1, 2000

[4] W. Wehl et al., Proc. IMAPS 2003

[5] D. Schuhmacher et al. *Proc. IEEE MEMS 2007*, pp. 357-360

[6] P. Sen and C. J. Kim, *Proc. IEEE MEMS 2007*, pp. 767-770

[7] T. Metz, et al. *Langmuir*, pp. 9204-9206, 2008

[8] ESI-Group, "CFD-ACE+ 2007," 2006

[9] S. L. Anna et al., *Appl. Phy. Let.* vol., 82, no. 3, pp. 364-366, Jan.2003.